Smooth 2D Coordinate Systems on Discrete Surfaces

Colin Cartade[1], Rémy Malgouyres[1], Christian Mercat[2], and Chafik Samir[3]

[1] Clermont-Université, LIMOS, Complexe des Cézeaux, 63172 Aubière, France
{colin.cartade,remy.malgouyres}@u-clermont1.fr
[2] Université Lyon 1, IUFM, Bât. Braconnier, 69622 Vileurbanne, France
christian.mercat@gmail.com
[3] Clermont-Université, ISIT, Complexe des Cézeaux, 63172 Aubière, France
chafik.samir@u-clermont1.fr

Abstract. We introduce a new method to compute conformal parameterizations using a recent definition of discrete conformity, and establish a discrete version of the Riemann mapping theorem. Our algorithm can parameterize triangular, quadrangular and digital meshes. It can be adapted to preserve metric properties. To demonstrate the efficiency of our method, many examples are shown in the experiment section.

Keywords: parameterization, conformal, digital surfaces.

Introduction

Knowing a parameterization of a surface is very useful because it allows to work with functions instead of three dimensional sets. Thus, we can easily apply real analysis results to surfaces. Moreover, as parameterizations establish a correspondence between a surface and a part of the plane, we can then extend planar techniques to surfaces. For all these reasons, they are widely used in mesh processing: among the many applications, we can cite texture mapping, morphing, surface fitting, etc.

A parameterization should preserve the geometrical properties of the mesh: angles (conformal map), areas (authalic maps), lengths (isometric map), etc. But maps which are both conformal and authalic maps are isometric, and only developable surfaces have an isometric flat parameterization. In practice, people often look for conformal maps. They preserve angles, lengths ratios locally, and more generally the local aspect of the mesh. It is often sufficient to obtain a good parameterization.

In this paper we present a new algorithm to compute conformal parameterizations using the definition of discrete conformity given in [10]. Although, it was first used for meshes, with floating point coordinates, it has the main advantage of being easily adaptable to digital surfaces, with integer coordinates. We show that, in the case of triangular meshes, it is a generalization of the *cotan* conformal coordinates method [13] and establish a discrete version of the Riemann

I. Debled-Rennesson et al. (Eds.): DGCI 2011, LNCS 6607, pp. 59–70, 2011.

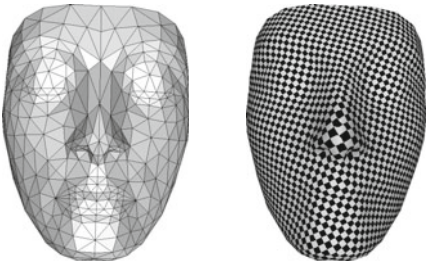

Fig. 1. Triangular mesh parameterization, $E = H + L'$ (see p. 67)

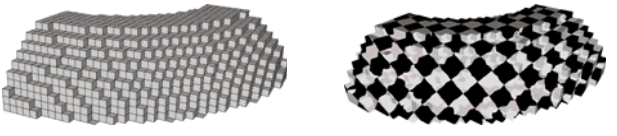

Fig. 2. Digital torus parameterization

mapping theorem. The boundary conditions introduced are closer to the real continuous theorem than those of classical conformal methods.

Our algorithm consists in minimizing a discrete energy to measure conformity. It can be generalized to preserve other properties such as faces areas and/or edges lengths allowing to obtain a more isometric parameterization. These energies can also be used to obtain parameterizations with free-boundary conditions as detailed in [4,8,9,14] and give better results around the boundary.

The rest of the paper is organized as follows. Section 1 introduces the definition of discrete conformal maps for quad meshes and show how it can be generalized to digital surfaces and triangular meshes. In Section 2, we explain how to choose boundary conditions, *i.e.* fix the position of some boundary points, to ensure uniqueness. We mainly focus on the two choices which lead to a discrete version of the Riemann mapping theorem and to the same parameterization as the *cotan* conformal coordinates. In Section 3, we describe precisely how we proceed in practice to compute parameterizations. Numerical illustrations are given in Section 4.

1 Discrete Conformal Parameterizations

1.1 Quad Meshes

In real continuous theory, a surface parameterization is a bijective application from the surface S in $\mathbb{R}^3$ to the plane: $(x, y, z) \in S \mapsto \big(s(x, y, z), t(x, y, z)\big) \in \mathbb{R}^2$. For meshes, it boils down to a point $v' = (s, t)$ assigned to each vertex $v = (x, y, z)$. In the sequel, we will identify v' with the complex number $s + it$.

Locally identifying each face (v_0, v_1, v_2, v_3) of a quad mesh to points in the plane (in one way or another) we can view the diagonals $v_2 - v_0$ and $v_3 - v_1$

as two complex numbers and compute the ratio $\rho = \frac{v_3 - v_1}{i(v_2 - v_0)}$, which is defined up to a global similarity. Following [10], we call this data a *discrete conformal structure* and we say that a parameterization is *discrete conformal* if it preserves the ratios ρ. In other words, for all faces of the mesh, we require that

$$\frac{v'_3 - v'_1}{v'_2 - v'_0} = i\rho. \tag{1}$$

Geometrically, such a parameterization preserves the angle between the diagonals and the ratio of their lengths. It is a property we expect since faces are small with respect to the whole mesh and a conformal map locally preserve angles and lengths ratios (its derivative is a similarity), For simplicity, we can rewrite (1) as a linear equation

$$v'_3 - v'_1 = i\rho(v'_2 - v'_0), \tag{2}$$

consequently a conformal parameterization can be seen as a solution of a (complex valued) linear system.

Remark 1. Even if the four vertices of a quad are not in the same plane we can define the ratio ρ. Indeed, the diagonals in $\mathbb{R}^3$, when not colinear, can be viewed as two vectors spanning a plane, wherein the complex ratio can be computed. This choice amounts to defining the normal to the surface as the cross-product of these diagonals. A prior knowledge of the normal, therefore of the tangent plane, is another way to identify the quad-face to a quadrilateral in the complex plane, by projecting the vertices onto this tangent plane. The ratio does not depend on the choice of the normal basis identifying the tangent plane with the complex numbers. Together, all these identifications of the tangent plane at each quad, considered as local charts, form an *atlas* of the surface.

1.2 Triangular Meshes

In general, faces of meshes are not quads but triangles and the definition extends to this case: we add a new (combinatorial) *dual point* to each face and to each boundary edge, a standard procedure in remeshing. Then for each edge of the initial mesh we form a quad by joining the extremities of the edge and

- the two dual points inside the adjacent faces if it is not a boundary edge
- the dual points inside the adjacent face and on the edge if it is a boundary edge.

The construction is shown in Figure 3. On the left, we display the initial triangular mesh and the dual points, and on the right the new quad mesh.

By definition, quads consist of two triangles that do not necessarily belong to the same plane. To determine the ρ coefficient, we rotate one of them until it belongs to the plane of second, that is to say we flatten them using the *intrinsic* metric of the polyhedral surface. Once we have this quad structure and a ρ for each quad we can look for a parameterization in the same way as in Section 1.1. Thus we parameterize not only the initial vertices but also the dual points.

The use of the extrinsic or intrinsic distances does not seem to imply big differences as noted in another context in [2].

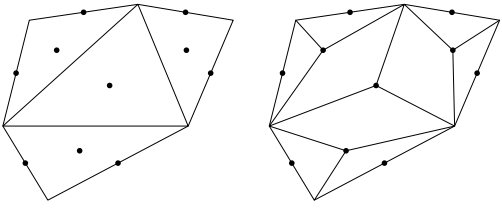

Fig. 3. Introduction of dual points

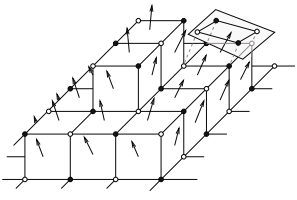

Fig. 4. Definition of ρ for digital surfaces

1.3 Digital Surfaces

The definition we gave in the previous section is not interesting as such when using digital surfaces whose faces are surfels. Indeed, these faces are planar squares and all the ρ coefficients equal 1. Therefore a more meaningful discrete conformal structure has to be defined, using *extrinsic* or non local data such as a given normal vector [11]: we compute a normal vector of each face using for instance the method described in [6], or coming from the scanned data. It allows us to determine the tangent plane of the surface in each surfel. Firstly, we project the four edgels on this plane, obtaining a parallelogram which better approximates the continuous surface than the initial surfel. Secondly we define the ρ coefficient of a surfel as the one of this projected parallelogram. An example of the construction is depicted in Figure 4.

2 Boundary Conditions

2.1 Solutions of the System

The linear system (2) does not have a unique solution since there are more unknowns than equations: If we denote by n_f, n_e, n_b and n_v the number of faces, edges, border edges and vertices of the mesh, it consists of $2n_f$ real equations and has $2n_v$ real unknowns. We have on the one hand (Euler characteristic of the disc)

$$1 = n_f - n_e + n_v, \tag{3}$$

and on the other hand (mesh property)

$$4n_f = 2n_e - n_b. \tag{4}$$

Adding $2 \times (3)$ to (4) we obtain

$$2(n_v - n_f) = n_b + 2.$$

Hence, in order to ensure uniqueness we need $n_b + 2$ real constraints.

2.2 Connection to Real Continuous Theory

The Riemann mapping theorem states that each surface homeomorphic to the closed disc is in fact conformally equivalent to the closed disc. Besides the holomorphic map is unique if one boundary is mapped to the other one and the images of 3 boundary points are fixed [1,16,3,7].

In the same way, we can map the boundary of the mesh to the unit circle. Thus we obtain n_b additional real constraints. Then, if we fix the images of two of the boundary vertices, we have the

$$(n_b - 2) + (2 \times 2) = n_b + 2$$

real constraints we are looking for.

This leads to the following discrete version of Riemann mapping theorem: if two (almost three) boundary vertices are fixed, there exists only one discrete conformal parameterization whose boundary points belong to the unit circle. These boundary points are not different from other boundary points. Our boundary conditions are much closer to the Riemann theorem than those of other classical discrete conformal algorithms: [5,13] fix all the boundary points and [4,9] fix two boundary points (that accumulate conformal distortion) but the other ones are not mapped on the circle.

2.3 Connection to the *cotan* Conformal Coordinates

In this section, we will show that our method is a generalization of parameterizations with the *cotan* conformal coordinates [4,13]. We remind the reader that this method applies to triangular meshes and consists in

1. fixing the images of the boundary points, often on a convex boundary,
2. solving the following system:
   for each vertex v_i which is not on the boundary of the mesh

$$\sum_{j\,:\,v_j \text{ neighbour of } v_i} \big(\cot \alpha_{ij} + \cot \alpha_{ji}\big)(v'_j - v'_i) = 0 \tag{5}$$

   (the angle α_{ij} and α_{ji} are defined on Figure 5, left picture).

Suppose that in the construction of dual points described in Section 1.2 we add the circumcenter of the triangles and the middle of the boundary edges. Consider two adjacent triangles faces (v_0, v_1, v_2) and (v_0, v_3, v_1). We denote by v_3 and v_4 their circumcenters and by c the middle of $[v_0, v_1]$. An example of the

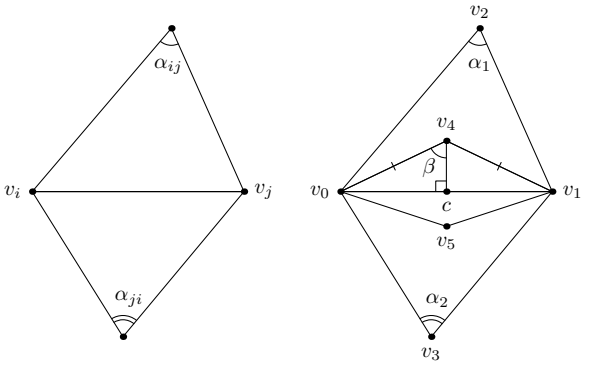

Fig. 5. Definition of the angles in the *cotan* formula

construction is shown in Figure 5 (right picture). We want to compute the ρ coefficient of the quad (v_0, v_5, v_1, v_4).

First, since the angle in c is right, ρ is real:

$$\rho = \frac{\|v_4 - c\|}{\|v_1 - v_0\|} + \frac{\|v_5 - c\|}{\|v_1 - v_0\|}.$$

Second,

$$\frac{\|v_4 - c\|}{\|v_1 - v_0\|} = \cot\beta = \cot\alpha_1.$$

since the triangle (v_0, c, v_4) is right in c (first equality) and $\alpha_1 = \frac{v_0\widehat{v_4}v_1}{2}$ according of the inscribed angle theorem (second equality).
Finally

$$\rho = \cot\alpha_1 + \cot\alpha_2.$$

Note that the coefficients are the same as in (5).

We denote by $\rho(v_i, v_j)$ the ρ coefficient of the quad containing the diagonal $[v_i, v_j]$. Adding the equations in (2) involving a particular initial vertex v_i we obtain

$$\sum_{j\ :\ v_j \text{ neighbour of } v_i} \rho(v_i, v_j)(v'_j - v'_i) = 0$$

It is in fact the sum over the dual edges which form a loop. Hence the system (2) is equivalent to a system which has (5) as a subsystem.

Due, to the results of section 2.1 we have to add $\frac{n_b}{2} + 1$ real constraints to ensure uniqueness. We choose to fix the initial boundary points (those of the triangular mesh) and one of the dual boundary points. Hence the coordinates v'_i of the initial mesh satisfy the same linear system as with *cotan* conformal coordinates and we obtain the same solution.

We have proved that our method is a generalisation with arbitrary dual points and boundary constraints of the *cotan* conformal coordinates. It can be of interest when some angles of the triangles are obtuse. Then the circumcenters are

not necessarily inside the triangles and the coefficients in (5) can be negative. Thus conditions of Tutte theorem [15] are not verified and the *cotan* conformal coordinates method can fail.

3 Practical Computation

3.1 Energy Minimization

Many parameterizations methods, including [4,5,9,13], consist in solving sparse linear systems. As the system of equations (2) is also sparse, we could think of using similar techniques. But the boundary condition, *i.e.* remaining on a circle, is not linear and even not quadratic. That is why we implement a non-linear minimization technique.

We denote by $\rho(v_i, v_j)$ the ρ coefficient of the face containing the diagonal $[v_i, v_j]$. Then we introduce the conformal energy

$$H = \sum \left| (v'_l - v'_j) - \rho(v_i, v_k)\big(v'_k - v'_i\big) \right|^2$$

where the sum is over all the quads (v_i, v_j, v_k, v_l) of the mesh,
and the boundary energy

$$C = \sum \left(|v'_i|^2 - 1 \right)^2$$

where the sum is over all the boundary vertices v_i except the two ones whose parameters are fixed. We search the parameters v'_i which minimize the total energy

$$E = \alpha H + \beta C$$

for chosen positive real numbers α and β. The minimization is performed using a conjugate gradient method (Fletcher-Reeves algorithm, [12]).

3.2 Initial Conditions

The minimization algorithms we use are guaranteed to converge to a local minimum but not necessarily to the global one. It is a very important issue in this case since there is no uniqueness in the Riemann theorem if the map is not one to one. For example, the one to one parameterization of the unit disc with three fixed points is the identity map. However, with convenient initial conditions our algorithm can perfectly lead to a discrete approximation of the $z \mapsto z^2$ map.

In practice, it works quite well to set at the beginning the images of the boundary points on a circle with the same distances between them as on the boundary of the mesh. And we set the initial positions of the images of the interior points at the origin. The algorithm more or less acts like the relaxation of a network of springs. We must also mention that in order to have less distortion it is generally better to choose the fixed points as far as possible from each other. For example when we fix two points, we try to select points with around half of the boundary length between them. An example is given in Figure 6 where the fixed points are represented by big dots.

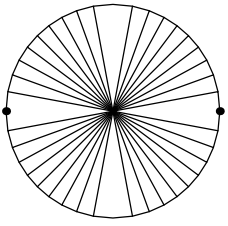

Fig. 6. Example of initial configuration

3.3 Preservation of Lengths and Areas

Yet, we focused on computing conformal maps to preserve angles and thus shapes locally. It is certainly a key feature in mesh parameterization but not enough to ensure a good result. Indeed, conformal maps can lead to parameterizations which are very tight in some regions and more sparse in others. If we map a checkerboard with such a parameterization we obtain big squares in the first regions and little ones in the others which is of course unsatisfactory.

To avoid these artifacts we define new energies attached to preserving metric properties such as:

1. the area of the faces,
2. the length of the edges.

First, we introduce the *authalic* energy

$$A = \sum \Big(\mathrm{Im}\left((v'_k - v'_i)\overline{(v'_l - v'_j)}\right)^2 - \left(\|(v_l - v_i) \wedge (v_k - v_i)\| + \|(v_k - v_i) \wedge (v_j - v_i)\|\right)^2 \Big)^2$$

where the sum is over all the quads (v_i, v_j, v_k, v_l) of the mesh,
and we secondly define the *metric* energy

$$L = \sum \left(|v'_i - v'_j|^2 - \|v_i - v_j\|^2\right)^2 \tag{6}$$

where the sum is over all the edges $[v_i, v_j]$. Then, we consider the energy

$$E = \alpha H + \beta A + \gamma L.$$

There are many more equations and we are no longer looking for a unique solution of a system but rather for the minimum of an energy. However, as any isometric transformation of a given parameterization has the same energy, we ensure uniqueness by fixing the image of one boundary point and the direction of the next boundary edge.

Note that such a minimal energy parameterization will not be conformal, unless the surface is developable. Indeed a map preserving both angles and areas is isometric and only developable surface have an isometric flat parameterization.

But choosing the coefficient α, β and γ conveniently we can obtain more accurate results. Moreover, as there is no longer a condition on the boundary we also obtain a more "natural" boundary, adapted to the mesh. The choice moved from the boundary points to the coefficients.

It can be quite slow to compute the energy L (and also A). To speed up our algorithm, we can minimize only the distortion of the metric along the boundary. Thus we introduce the metric energy L' defined as (6) where the sum is over the boundary edges only. It allows us to obtain a conformal map with a more "natural" boundary, closer to another classical Riemann-Hilbert condition [16]. Note also that even with the initial conditions described in the previous section, in general, for numerical reasons, the algorithm does not converge towards the right local minimum if we do not use the energy C. It does, however, if we use the following two steps process:

1. minimize H with a fixed boundary.
2. use this minimum as initial condition to minimize E.

Moreover, as the minimization is very fast when we fix all the boundary points, it also speeds up the convergence.

4 Results

4.1 Comparison of the Energies

We first computed parameterizations of the mesh $(s,t) \mapsto \cos(s) + \cos(t)$ (discretized with quad faces) to show the main advantages and drawbacks of each of the energies C (circle), L' (length of the boundary), L (length) and A (area). You can see the corresponding results in Figure 7, 8, 9 and 10. Additionally, the algorithm can be applied on triangular meshes as shown in Figure 1.

The parameterizations are displayed on the left. On the right, we mapped a 32×32 checkerboard on the surface using this parameterization. With the circle boundary energy $E = H + C$ (Figure 7), we obtain a conformal parameterization (the shape of the squares is preserved) but the behavior around the boundary is not natural (because a circle is very different from the true boundary of the mesh). In particular there is a big distortion of the metric in this region. If we use the boundary metric energy L' instead of C (Figure 8), the map is still conformal but the boundary is better preserved. We observed that the results are visually quite close to those of other methods with free boundary (ABF, circle patterns, etc.). The use of the energies L and A has the same effect on the boundary. Besides, even if the parameterization is not conformal (see all the red points in Figure 7), the texture mapping looks more accurate since all the squares have the same size. However, close inspection shows that some squares of the checkerboard become rectangles after the mapping.

4.2 Digital Surfaces

We also computed parameterizations of digital surfaces. We used a digital torus consisting of around 1500 surfels. We first computed a parameterization using

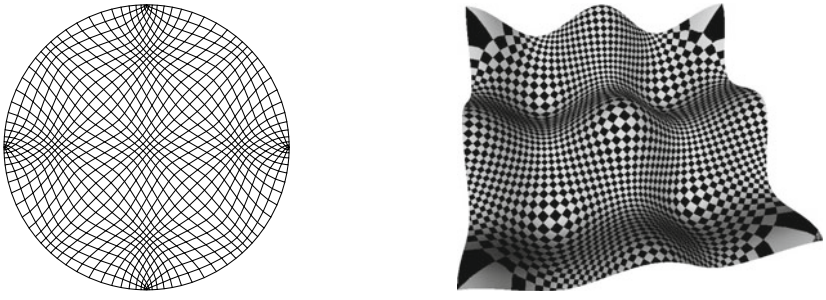

Fig. 7. $E = H + C$, circle boundary

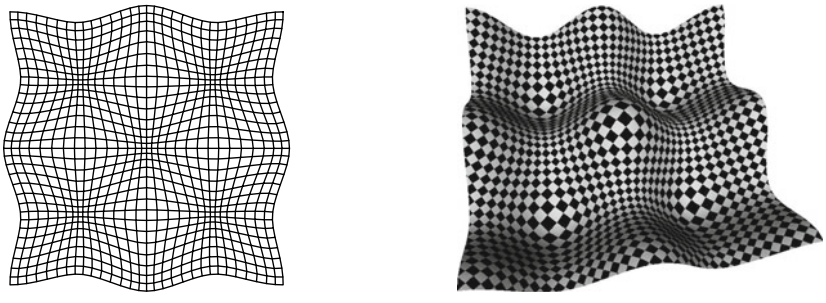

Fig. 8. $E = H + L'$, more isometric along the boundary

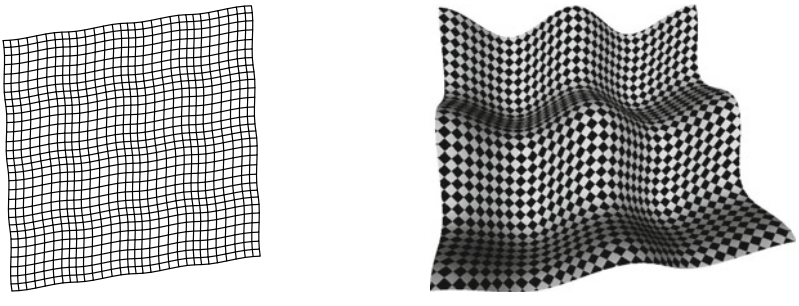

Fig. 9. $E = H + L$, more isometric

Fig. 10. $E = H + A$, more area preserving

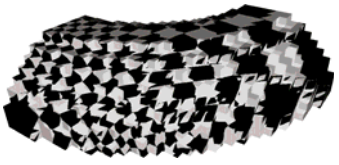

Fig. 11. Method for quad meshes with digital normal, $E = H + C$

(a) (b)

Fig. 12. Digital method with smoothed normal, (a) $E = H + C$, (b) $E = H + A$

the method for quad meshes without smoothing the normal. As expected the resulting texture mapping is not good: we do not even distinguish the checkerboard squares in some regions of Figure 11. Then we use our method for digital surfaces and obtain better results: we clearly distinguish the checkerboard on Figure 12. This figure also shows that the influence of additional energies is the same as with float meshes.

5 Conclusion and Future Work

We have described a new method of conformal parameterization that can be applied to different meshes, including triangular meshes and digital surfaces. As a proof of concept, we have used different cost functions whose minimum preserves more or less the shape, the size, and the boundary conditions. An important feature of our approach is the introduction of a recent definition of discrete conformity allowing many possibilities for more accurate results. We have shown various experimental results to illustrate the different possibilities. In future work, we will study the choice of coefficients α, β, etc. In particular, it would be interesting to compute the more isometric conformal parameterization.

Acknowledgement. This work was partially supported by the ANR project KIDICO (ANR-2010-BLAN-0205-02).

References

1. Ahlfors, L.V.: Complex analysis, 3rd edn. McGraw-Hill Book Co., New York (1978); an introduction to the theory of analytic functions of one complex variable, International Series in Pure and Applied Mathematics
2. Bobenko, A.I., Mercat, C., Schmies, M.: Conformal Structures and Period Matrices of Polyhedral Surfaces. In: Computational Approach to Riemann Surfaces. Springer, Heidelberg (2011)

3. Bobenko, A.I., Schröder, P., Sullivan, J.M., Ziegler, G.M. (eds.): Discrete differential geometry, Oberwolfach Seminars, vol. 38. Birkhäuser, Basel (2008), http://dx.doi.org/10.1007/978-3-7643-8621-4 (papers from the seminar held in Oberwolfach, May 30-June 5, 2004)
4. Desbrun, M., Meyer, M., Alliez, P.: Intrinsic parameterizations of surface meshes. Computer Graphics Forum 21, 209–218 (2002)
5. Floater, M.S.: Mean value coordinates. Computer Aided Geometric Design 20(1), 19–27 (2003)
6. Fourey, S., Malgouyres, R.: Normals estimation for digital surfaces based on convolutions. Computers & Graphics 33(1), 2–10 (2009)
7. Gu, X.D., Yau, S.T.: Computational conformal geometry, Advanced Lectures in Mathematics (ALM), vol. 3. International Press, Somerville (2008); with 1 CD-ROM (Windows, Macintosh and Linux)
8. Kharevych, L., Springborn, B., Schröder, P.: Discrete conformal mappings via circle patterns. ACM Transactions on Graphics (TOG) 25(2), 438 (2006)
9. Lévy, B., Petitjean, S., Ray, N., Maillot, J.: Least squares conformal maps for automatic texture atlas generation. ACM Transactions on Graphics 21(3), 362–371 (2002)
10. Mercat, C.: Discrete Riemann surfaces and the Ising model. Communications in Mathematical Physics 218(1), 177–216 (2001)
11. Mercat, C.: Discrete complex structure on surfel surfaces. In: Coeurjolly, D., Sivignon, I., Tougne, L., Dupont, F. (eds.) DGCI 2008. LNCS, vol. 4992, pp. 153–164. Springer, Heidelberg (2008)
12. Nocedal, J., Wright, S.J.: Numerical optimization. Springer, Heidelberg (1999)
13. Pinkall, U., Polthier, K.: Computing discrete minimal surfaces and their conjugates. Experimental Mathematics 2(1), 15–36 (1993)
14. Sheffer, A., de Sturler, E.: Parameterization of faceted surfaces for meshing using angle-based flattening. Engineering with Computers 17(3), 326–337 (2001)
15. Tutte, W.: Convex representations of graphs. Proceedings of the London Mathematical Society 3(1), 304 (1960)
16. Wegert, E.: Nonlinear Riemann-Hilbert problems—history and perspectives. In: Computational Methods and Function Theory 1997 (Nicosia), Ser. Approx. Decompos., vol. 11, pp. 583–615. World Sci. Publ., River Edge (1999)